AL KUT JOURNAL OF ECONOMIC AND ADMINISTRATIVE SCIENCES
Publisher: College of Economics and Management - Wasit University

# Developing Models Inspired by CNN and DNN for more Effective Precipitation Forecasting Techniques

https://doi.org/10.29124/kjeas.1651.17

**Waleed Ahmed Hassen Al-Nuaami**

Biology department, Collage of pure science, Diyala University, Diyala, Iraq

purecomp.waleed.hassan@uodiyala.edu.iq

## Abstract

The study aims to analyze some changes in rainfall behavior in (10) global cities, including Tokyo, Osaka, Shanghai, Chicago, Istanbul, Buenos Aires, Amsterdam, Madrid, Florance, and New York using an advanced machine learning (ML) approach for predicting the average precipitation. Utilizing the Deep Neural Network (DNN) and Convolution Neural Network (CNN) model, we have acquired mean precipitation monthly data from the selected cities with covering the period of 2000-2023. In order to assess mean precipitation in cities, we effectively employed both the average mutual information (AMI) during the model's development. Constructed using both a training subset (80% of data from 2000 to 2018) and a testing subset (20% of data from 2019 to 2023), MP forecasting models for ten cities were established. When compared to the DNN model, the CNN model truly shined by showcasing its remarkable potential as a high-level model in accurately estimating mean precipitation values of cities while demonstrating superior generalization ability and minimal variance.

**Keywords:** Convolution Neural Network, City mean precipitation, forecasting, Deep Neural Network

## Graphical Abstract

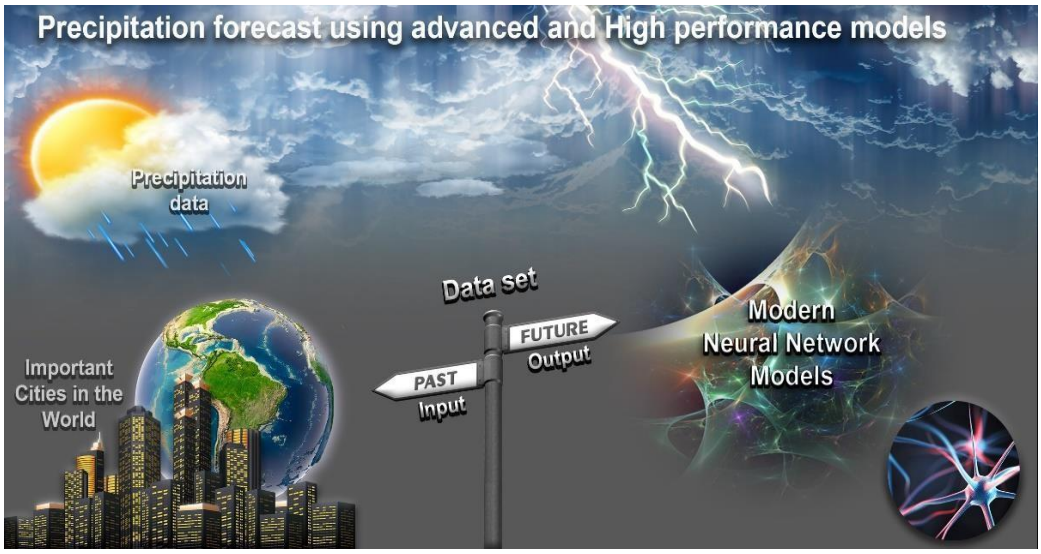


## 1. Introduction

Scientists have been attracted to the development of drought prediction models for mitigating impacts, as there has been a noticeable increase in drought frequency and severity worldwide caused by climate change. Weather forecasting predicts future weather conditions such as precipitation, temperature, pressure, and wind and is fundamental to science and society (Sønderby et al. 2020). The forefronts of physical modeling and computing technology merge within this field to form a unified scientific and technological endeavor spanning a hundred years (Bauer et al. 2015). It is very important to obtain the stability of the orderly management of water and to be careful of flooding Determine the elements of the air and the location of the water, ocean currents, and human activities contribute to the complexity of this nonlinear system (Maheswaran et al. 2014).

There is an urgent need to estimate the amount of rain that will start in the future (Qiu et al. 2018; Chau et al. 2010). There is a great reliance on classical methods in estimating the amounts of rain. With their roots in Lagrang echo extrapolation (Pulkkinen et al. 2020; Woo et al. 2017), traditional nowcasting models have been enhanced in recent times to estimate precipitation growth and decay (Ryu et al. 2020; Foresti et al.

2019) with forecasts of the amount of rain (Nerini et al. 2020; Chung et al. 2020).. Their primary aim was to advance precipitation nowcasting compared to extrapolation models by altering the LSTM with convolution operators in both state-to-state and input-to-state. While the statistical model proves beneficial due to its minimal computational requirements, it lacks proficiency in accurately predicting complex series, therefore in recent years, the utilization of artificial intelligence prediction models in precipitation forecasting research has been extensive (Li et al. 2020). Papacharalampous et al. (2019) compared the application of artificial intelligence models in hydrological time series forecasting.

Although singleton AI methods for time series prediction are meant to be flexible, previous studies indicated that their effectiveness is limited when it comes to long-term rainfall prediction, especially in semiarid and arid regions (Kisi and Cimen. 2012; Nourani et al. 2009). Machine learning focuses on the problem of creating computers that can enhance their performance through accumulated experience without external intervention. In multi-disciplinary technologies, data-intensive science has been revolutionized by the collaboration between big data technologies and high-performance computing, transforming it with machine learning (Liakos et al. 2018). For forecasting purposes, a wide range of artificial intelligence, machine learning (ML), and deep machine learning (DML) algorithms have been developed to model linear and nonlinear complex hydrological systems, climate science, and agricultural production effectively and efficiently. Artificial intelligence has been frequently applied for forecasting of daily river discharge and stream flow (Lohani et al. 2006; Rezaie-Balf et al. 2017; Sammen et al. 2021), rainfall and runoff (Ridwan et al. 2021), forecasting of the hydrological event annual precipitation trends (Dash et al. 2018; Malik et al.

The present research examines the proficiency of the (Deep Artificial Neural Network) DNN and (Convolution neural network) CNN models in accurately forecasting monthly mean precipitation, owing to the exceptional data-capturing capabilities of the DNN and CNN algorithms. Researchers have fewer studies on using the DNN and CNN techniques for predicting fluctuations in the mean precipitation of cities. Therefore, the objective of this research is to reliably forecast the Mean Precipitation (MP) fluctuations in the ten most important cities in the world namely: Tokyo, Shanghai, New York, Madrid, Amsterdam, Chicago, Istanbul, Osaka, Buenos Aires, and Florence using the standalone DNN and CNN models.

## 2. Materials and Methods

### 2.1. Study area and data required

In cities, rainfall holds great importance as it affects numerous aspects of urban life like water supply, infrastructure, and the environment. This phenomenon can be attributed to various factors including city shape, the impact of urban heat islands, and a rise in urban aerosols. The study region selected for forecasting multistep mean precipitation is ten important cities in the world, which is situated location and general information in Table 1 and **Fig. 1**.

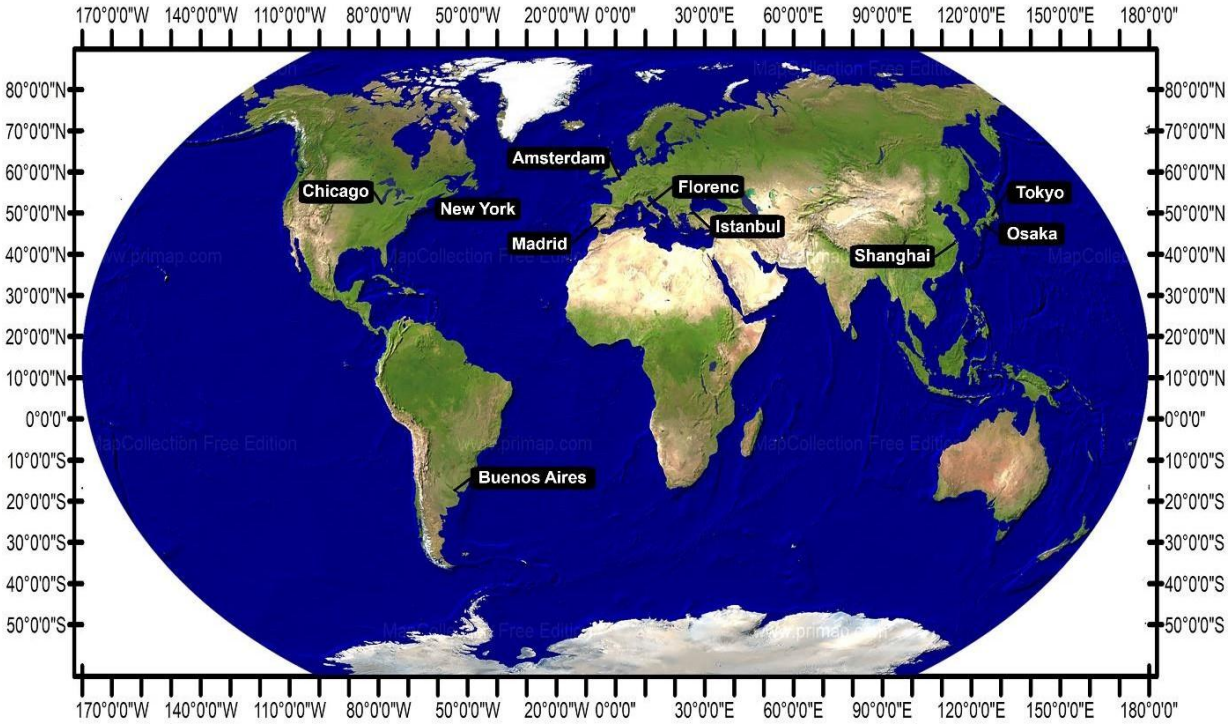


**Fig. 1** The location of the ten most important cities in the world

**Table 1.** General information of the ten cities selected in this research

| Cities | Location | a Level (m) | Area ($km^2$) | opulation (People) |
|---|---|---|---|---|
| Tokyo-Japan | 35.67° N, 139.65° E | 40 | 2194 | 13617445 |
| Osaka-Japan | 34.69° N, 135.50° E | 37.5 | 223 | 2713157 |
| Shanghai-China | 31.23° N, 121.47° E | 4 | 6340 | 24152700 |
| New York-USA | 40.71° N, 74.01° W | 10 | 783.8 | 8804190 |
| Chicago-USA | 41.87° N, 87.62° W | 182 | 600 | 2746388 |

| | | | | |
|---|---|---|---|---|
| Amsterdam-Netherlands | 52.36° N, 4.90° E | 2 | 219.3 | 851573 |
| Madrid-Spain | 40.41° N, 3.70° W | 657 | 604.3 | 3165541 |
| Istanbul-Turkey | 41.01° N, 28.97° E | 40 | 5461 | 14804116 |
| Buenos Aires-Argentina | 34.60° S, 58.38° W | 25 | 203 | 2890151 |
| Florence-Italy | 43.76° N, 11.25° E | 50 | 102.4 | 382258 |

To assess the proposed models, this study specifically chose Tokyo, Shanghai, New York, Madrid, Amsterdam, Chicago, Istanbul, Osaka, Buenos Aires, and Florence as the cities to evaluate based on the MP time series data with both high and low variations. The US NOAA and Mathematica software databases were used to collect the Mean Precipitation data monthly for 2000 to 2023 in these cities. The statistical characteristics of the collected Mean Precipitation data for ten crucial cities are different, as shown in Table 2. To create a model, the mean precipitation data sets were partitioned, allocating 80% for training purposes (2000 to 2018) and 20% for testing (encompassing the time frame of 2019 to 2023). **Fig. 2** shows the monthly mean precipitation values in ten cities from 2000 to 2023 (288 months).

**Table 2.** Statistical characteristics of the collected Mean Precipitation data for ten crucial cities

| **Cities** | **aximum (cm)** | **inimum (cm)** | **Iedian (cm)** | **Mean (cm)** |
|---|---|---|---|---|
| Tokyo | 77.98 | 0.05 | 11.47 | 13.45 |
| Osaka | 43.41 | 0.05 | 9.39 | 11.32 |
| Shanghai | 60.74 | 0.53 | 9.13 | 11.47 |
| New York | 43.71 | 0.02 | 7.98 | 8.54 |
| Chicago | 24.83 | 0.02 | 4.77 | 5.75 |
| Amsterdam | 25.71 | 0 | 6.26 | 6.97 |
| Madrid | 18.41 | 0 | 2.46 | 3.26 |
| Istanbul | 19.55 | 0 | 3.74 | 4.46 |
| Buenos Aires | 33.4 | 0 | 7.36 | 9.16 |
| Florence | 29.6 | 0 | 5.37 | 6.31 |

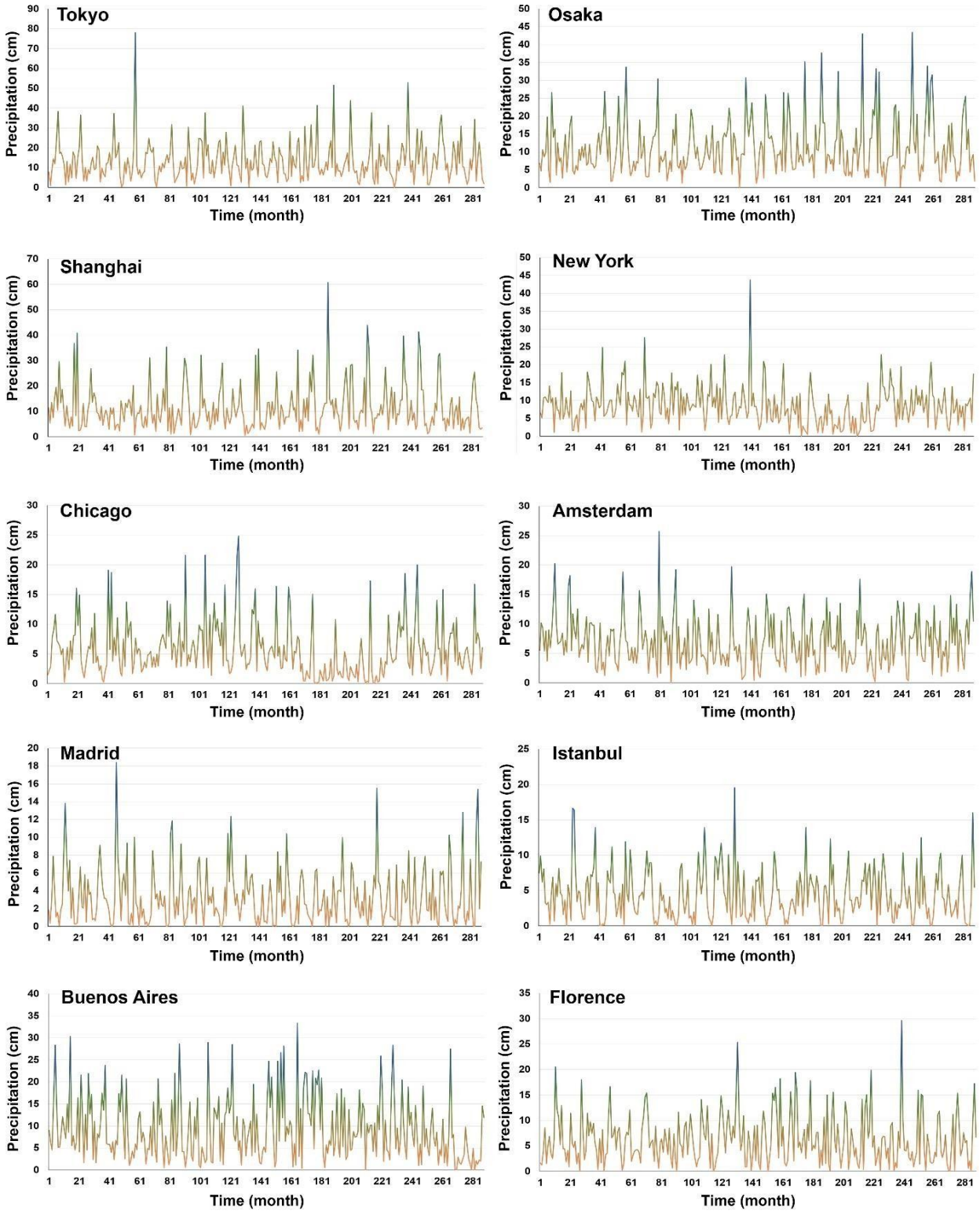


**Fig. 2** Temporal distribution of monthly mean precipitation time series for ten cities in the years 2000 to 2023

## 2.2. Deep Neural Network (DNN)

A Deep Artificial Neural Network (DNN) comprises multiple layers positioned between the input and output layers in an artificial neural network (ANN). Promising advancements have been made in constitutive modeling using Machine Learning methodologies, with a particular emphasis on Deep Artificial Neural Networks (DNNs). With no rules necessary, the neural network automatically extracts expert details from data, distinguishing it from traditional rule-based AI techniques (Ujong et al. 2022). To put it differently, by embracing a trial-and-error methodology, the system attains a high level of expertise in the field designated by the user. The DNN denotes a structure that emulates the way information is processed by the brain and nervous system in living organisms and an extensive assortment of interwoven processing elements (neurons) work collectively to ascertain a resolution to a precise problem (Wu et al., 2009; Park & Lee, 2011). Neurons are attached in a complex spatial arrangement.

In 1943, McCulloch and Pitts introduced the primary perceptron that is still used today by replicating the operational style of a living neuron (Ujong et al. 2022). In order for an artificial neural network to acquire knowledge and efficiently comprehend convoluted information, the activation function is indispensable and Its fundamental function lies in converting the input signal of a node in an artificial neural network to generate an output signal. The mathematical expression for the summation/transfer function for ANN is given in the following.

$$x_0 \cdot w_0 + x_1 \cdot w_1 + x_2 \cdot w_2 \ldots \; x_n \cdot w_2 = \sum x \cdot w_i \qquad (1)$$

x0, x1, x2, x3…x(n) represents various input parameters to the network, and the weights are represented as w0, w1, w2, w3… w(n). artificial neural network model as represented in **Fig. 3**.

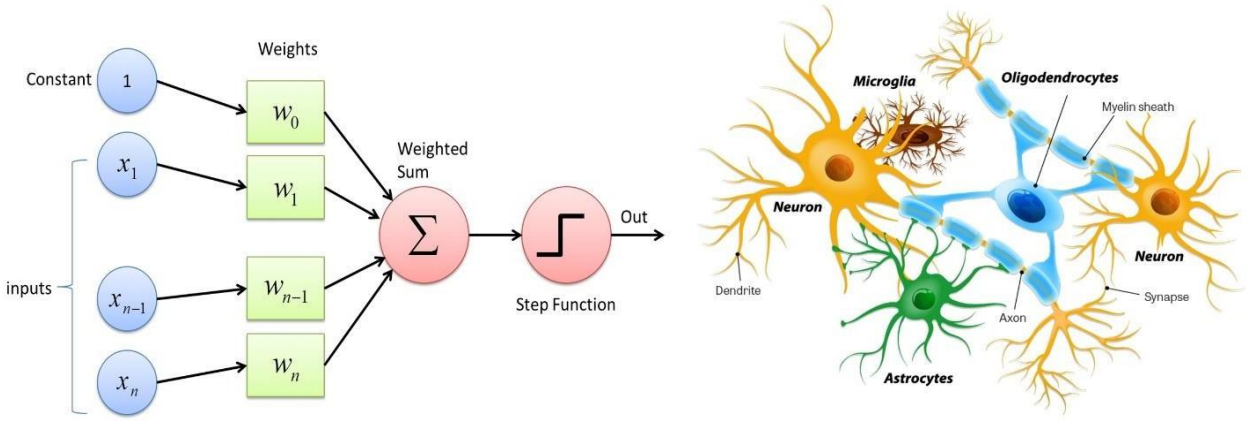


**Fig. 3** Deep artificial neural network model and biological neuron

## 2.3. Convolution Neural Network (CNN)

A Convolutional Neural Network (CNN) is a type of deep learning neural network architecture commonly used in computer vision tasks (O'Shea and Nash. 2015). Convolutional neural networks (CNNs), distinguished by their intricate network structures, surpass traditional machine learning methods in terms of feature learning and representation, displaying superior abilities (Krizhevsky et al. 2012). The acquisition of feature engineering in CNNs occurs automatically through filters or kernels and involves various layers such as input, convolutional, pooling, and fully connected layers. Convolutional Neural Networks (CNNs) have several advantages, including: (i) Highly accurate at data recognition and classification, (ii) Weight sharing, (iii) Minimizing computation and Ability to handle large datasets, (iv) Hierarchical learning and Applications (Milosevic et al. 2020). CNN has the advantage of utilizing a shared convolution kernel, which effectively processes high-dimensional data, automatically extracts advanced features, and reduces the need for manual feature engineering (Krizhevsky et al. 2012). The convolution neural network model is shown in **Fig. 4**.

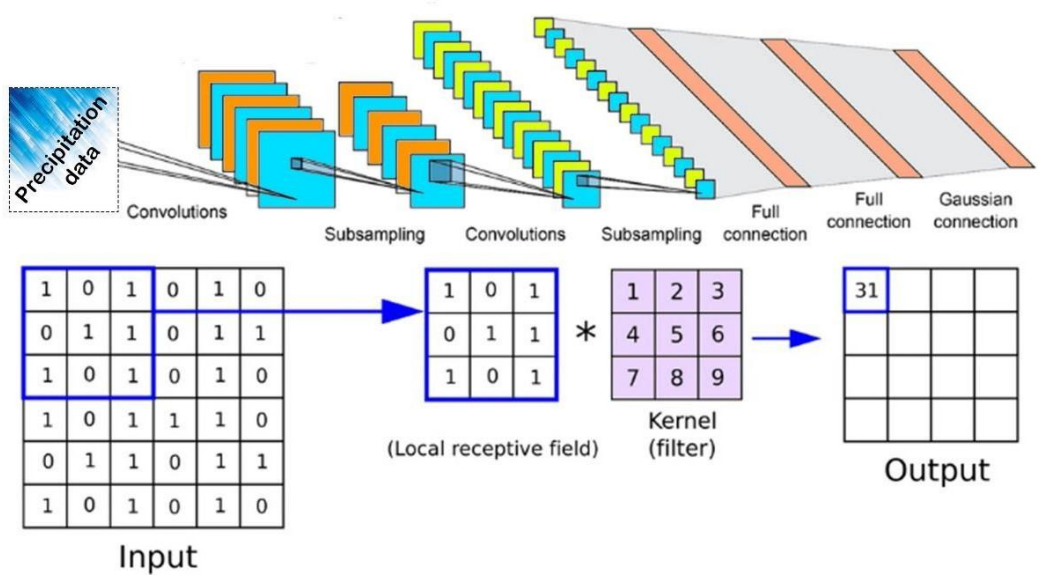


**Fig. 4** Different layers of convolutional neural network for prediction precipitation

## 2.4. Performance criteria

The assessment of modeling efficiency is performed by employing root mean square error (RMSE), correlation (R), and coefficient of determination ($R^2$) in both the training and testing stages:

$$R = \frac{\sum_{i=1}^{N} (MP_{oi} - \overline{MP}_o)(MP_{pi} - \overline{MP}_p)}{\sqrt{\sum_{i=1}^{N} (MP_{oi} - \overline{MP}_o)^2 \cdot \sum_{i=1}^{N} (MP_{pi} - \overline{MP}_p)^2}} \quad -1 \le R \le 1 \qquad (14)$$

$$R^2 = \left( \frac{N \sum_{i=1} (MP_{o,i} - \overline{MP}_o)(MP_{p,i} - \overline{MP}_p)}{} \right.$$

$$)^2 \qquad 0\leq R^2 \leq 1 \qquad (15)$$

$$\sqrt{\sum^{N} \left(\overline{M}^2 \sum^{N} \overline{M}^2\right.}$$

$$\Sigma$$

$$L$$

$$i=1 \quad o,i-M \quad . \quad i=1(ML_{p,i}-ML_p)$$

$$Lo)$$

---

$$RMSE = \sqrt{\frac{1}{}} \sum^{N} \quad (\quad - \quad)^2 \qquad 0\leq RMSE \leq \infty \qquad (16)$$

$$M \quad MP$$

$$P$$

$$N \quad i=1 \quad p,i \quad o,i$$

where, $MP_{p,i}$ and $MP_{o,i}$ indicate the estimated and observed data, $N$ refers to the number of data, and $\overline{MP}$ and $\overline{MO}$ are the average of the estimated and observed data.

## 3. Result

### 3.1. Model design and development

One way to differentiate time series forecasting techniques is by categorizing them as univariate or multivariate, depending on the number of variables available for observation. Employing the univariate forecasting method allowed for anticipation of upcoming MPs, based on the premise that previous values exclusively impact future values of the time series; this particular strategy may present advantages that go beyond those provided by multivariate time series forecasting. In general, the lower complexity of univariate time series forecasts leads to faster estimation when compared to their multivariate counterparts.

Careful selection of the input variables can greatly boost the effectiveness of a model within the realm of modeling. Also Choosing the best input variables for the output variable, also known as feature selection, is an essential step in machine learning to improve model performance and reduce computational cost. There are many mechanisms when deciding on optimization of variables output variable variables, such as gamma test and Method of average information exchanged, and the Average Mutual Information method (AMI) (Ghorbani et al 2022). To calculate the the time delay τ was carried out in this study through the use of the autoregression function with Use AMI technology.. Optimal values for delay (τ) at the city's mean precipitation can be determined by referring to **Fig. 5**, which demonstrates a correlation between the lowest AMI value and a delay of 3. The modeling of cities MP involves displaying distinct combinations of input variables derived from the AMI outcomes in Table 3.

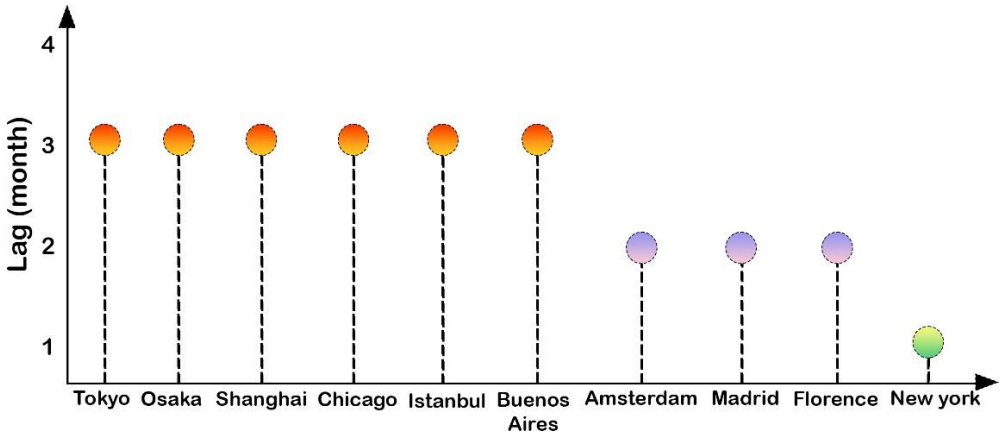


**Fig. 5** The Average Mutual Information ten important cities

**Table 3.** Selected combinations of input variable(s) for multistep ahead Mean Precipitation ten cities

| Cities | Scenario | Inputs | Output |
|---|---|---|---|
| Tokyo | M1 | MP(t) | MP(t) |
| | M2 | MP(t), MP(t-1) | MP(t) |
| | M3 | MP(t), MP(t-1), MP(t-2) | MP(t) |
| | M4 | MP(t), MP(t-1), MP(t-2), MP(t-3) | MP(t) |
| Osaka | M1 | MP(t) | MP(t) |
| | M2 | MP(t), MP(t-1) | MP(t) |
| | M3 | MP(t), MP(t-1), MP(t-2) | MP(t) |
| | M4 | MP(t), MP(t-1), MP(t-2), MP(t-3) | MP(t) |
| Shanghai | M1 | MP(t) | MP(t) |
| | M2 | MP(t), MP(t-1) | MP(t) |

| | | | |
|---|---|---|---|
| | M3 | MP(t), MP(t-1), MP(t-2) | MP(t) |
| | M4 | MP(t), MP(t-1), MP(t-2), MP(t-3) | MP(t) |
| New York | M1 | MP(t) | MP(t) |
| | M2 | MP(t), MP(t-1) | MP(t) |
| Chicago | M1 | MP(t) | MP(t) |
| | M2 | MP(t), MP(t-1) | MP(t) |
| | M3 | MP(t), MP(t-1), MP(t-2) | MP(t) |
| | M4 | MP(t), MP(t-1), MP(t-2), MP(t-3) | MP(t) |
| Amsterdam | M1 | MP(t) | MP(t) |
| | M2 | MP(t), MP(t-1) | MP(t) |
| | M3 | MP(t), MP(t-1), MP(t-2) | MP(t) |
| Madrid | M1 | MP(t) | MP(t) |
| | M2 | MP(t), MP(t-1) | MP(t) |
| | M3 | MP(t), MP(t-1), MP(t-2) | MP(t) |
| | M1 | MP(t) | Mp(t) |
| | M2 | MP(t), MP(t-1) | MP(t) |

| | | | |
|---|---|---|---|
| Istanbul | | | |
| | M3 | MP(t), MP(t-1), MP(t-2) | MP(t) |
| | M4 | MP(t), MP(t-1), MP(t-2), MP(t-3) | MWS (t) |
| | M1 | MP(t) | MP(t) |
| | M2 | MP(t), MP(t-1) | MP(t) |
| Buenos Aires | | | |
| | M3 | MP(t), MP(t-1), MP(t-2) | MP(t) |
| | M4 | MP(t), MP(t-1), MP(t-2), MP(t-3) | MP(t) |
| | M1 | MP(t) | MP(t) |
| Florence | M2 | MP(t), MP(t-1) | MP(t) |
| | M3 | MP(t), MP(t-1), MP(t-2) | MWS (t) |

Mathematica software determined the optimal parameters for the models during their training phase by analyzing and identifying the ideal mean precipitation input combination. MP values were predicted by employing statistical and visual analysis to assess the effectiveness of two standalone models (DNN and CNN). Table 4 provides a comprehensive representation of the performance criteria, such as coefficient of correlation (R) and root mean square error (RMSE), relevant to the testing period. Additionally, in Fig 6-10, you can observe the time series plots, Box plots, and Confidence bands of ten important cities during the testing phase.

**Table 3.** Performance criteria of the DNN and CNN models in the testing period for ten cities

| **Cities** | **Model** | **RMSE (cm)** | **R** | **Cities** | **Model** | **RMSE (cm)** | **R** |
|---|---|---|---|---|---|---|---|
| | CNN-M1 | 0.2562 | 0.9963 | | CNN-M1 | 0.1920 | 0.9920 |
| | CNN-M2 | 0.2174 | 0.9978 | | CNN-M2 | **0.1608** | **0.9988** |
| | CNN-M3 | **0.1598** | **0.9989** | | CNN-M3 | 0.2726 | 0.9947 |
| **Tokyo** | CNN-M4 | 0.1623 | 0.9989 | **Osaka** | CNN-M4 | 0.2801 | 0.9918 |
| | DNN-M1 | 1.5875 | 0.9859 | | DNN-M1 | 1.9855 | 0.9784 |
| | DNN-M2 | **1.4693** | **0.9898** | | DNN-M2 | 2.2108 | 0.9731 |
| | DNN-M3 | 1.5230 | 0.9873 | | DNN-M3 | 2.3429 | 0.9767 |
| | DNN-M4 | 1.8907 | 0.9875 | | DNN-M4 | **1.2860** | **0.9873** |
| | CNN-M1 | 0.1462 | 0.9977 | | CNN-M1 | 0.2185 | 0.9921 |
| | CNN-M2 | 0.1174 | 0.9980 | | CNN-M2 | **0.1455** | **0.9989** |

| | | | | | | | |
|---|---|---|---|---|---|---|---|
| | CNN-M3 | 0.1145 | 0.9984 | | CNN-M3 | 0.2806 | 0.9936 |
| **Shanghai** | CNN-M4 | **0.1134** | **0.9989** | **Chicago** | CNN-M4 | 0.1600 | 0.9985 |
| | DNN-M1 | 1.9107 | 0.9776 | | DNN-M1 | 1.8769 | 0.9453 |
| | DNN-M2 | 1.8827 | 0.9878 | | DNN-M2 | 2.4578 | 0.8646 |
| | DNN-M3 | **1.7876** | **0.9881** | | DNN-M3 | 1.7120 | 0.9713 |
| | DNN-M4 | 2.4405 | 0.9740 | | DNN-M4 | **1.4671** | **0.9838** |
| | CNN-M1 | 0.2313 | 0.9922 | | CNN-M1 | 0.2135 | 0.9943 |
| | CNN-M2 | **0.1023** | **0.9987** | | CNN-M2 | **0.1314** | **0.9988** |
| | CNN-M3 | 0.1609 | 0.9961 | | CNN-M3 | 0.1663 | 0.9957 |
| **Istanbul** | CNN-M4 | 0.1126 | 0.9976 | **Buenos Aires** | CNN-M4 | 0.1603 | 0.9958 |
| | DNN-M1 | 1.5429 | 0.9342 | | DNN-M1 | 1.7109 | 0.9559 |
| | DNN-M2 | 1.4648 | 0.9534 | | DNN-M2 | 1.6116 | 0.9564 |
| | DNN- | 1.6427 | 0.9133 | | DNN- | **1.4890** | **0.9796** |

| | | | | | | | |
|---|---|---|---|---|---|---|---|
| | M3 | | | | M3 | | |
| | DNN-M4 | **1.3767** | **0.9582** | | DNN-M4 | 2.3197 | 0.9462 |
| | CNN-M1 | 0.3965 | 0.9942 | | CNN-M1 | 0.3877 | 0.9966 |
| | CNN-M2 | 0.3727 | 0.9962 | | CNN-M2 | **0.1944** | **0.9990** |
| **Amsterdam** | CNN-M3 | **0.3433** | **0.9966** | **Madrid** | CNN-M3 | 0.1983 | 0.9981 |
| | DNN-M1 | 1.4362 | 0.9755 | | DNN-M1 | 1.5632 | 0.9483 |
| | DNN-M2 | **1.1649** | **0.9873** | | DNN-M2 | **1.1193** | **0.9807** |
| | DNN-M3 | 1.8239 | 0.9407 | | DNN-M3 | 2.0261 | 0.8662 |
| | CNN-M1 | 0.3864 | 0.9968 | | CNN-M1 | 0.1391 | 0.9893 |
| | CNN-M2 | **0.2533** | **0.9981** | | CNN-M2 | **0.1158** | **0.9987** |
| **Florence** | CNN-M3 | 0.2875 | 0.9979 | **New York** | DNN-M1 | 1.3890 | 0.9649 |
| | DNN-M1 | 1.7592 | 0.9623 | | DNN-M2 | **1.1897** | **0.9778** |
| | DNN-M2 | **1.6325** | **0.9838** | | | | |

| | | |
|---|---|---|
| DNN-M3 | 2.2293 | 0.9441 |

The findings from Table 3 reveal that within the realm of DNN models, the performance of DNN-M2 for Tokyo, Amsterdam, Madrid, Florence, and New York, DNN-M3 for Shanghai, Buenos Aires, and DNN-M4 for Chicago, Osaka, and Istanbul models proved to be good accurate during the testing phase. This is substantiated by its substantial R value between (0.958, 0989) and significantly reduced RMSE value between (1.787, 1.119), which were obtained through utilizing MP(t), MP(t-1), MP(t-2) ... MP(t-n) variables. Among the CNN models, CNN-M2 for Osaka, Chicago, Istanbul, Buenos Aires, Madrid, Florence, and New York, CNN-M3 for Tokyo, and Amsterdam, and CNN-M4 for Shanghai models estimate values with less error based on the most value of R between (0.996, 0.999) and lowest value of RMSE between (0.102, 0.253) in the testing stage using MP(t) variables. Consistently in every input scenario (M1-Mn), the performance of the CNN model proves to be superior to that of the DNN model, as revealed by the comparative analysis. **Fig. 6 and 7**, compares a time series graph of the best models of the DNN and CNN for ten selected important cities. The accurate performance and noticeable similarity between the CNN (M3 and M2) and DNN (M3 and M4) models can be observed in **Fig 6 and 7** through their time series graphs.

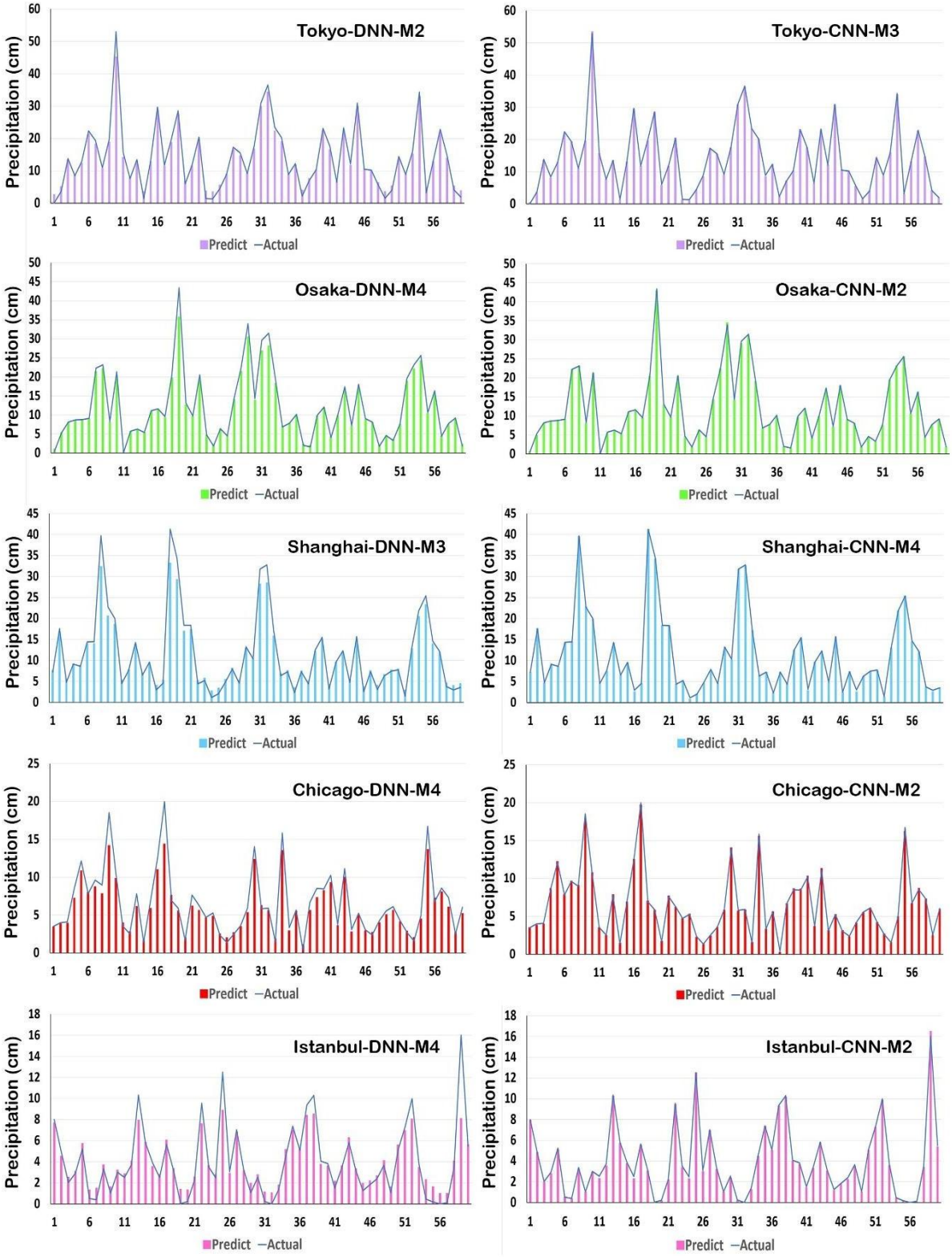


**Fig. 6** Time series for Tokyo, Osaka, Shanghai, Chicago, and Istanbul best DNN and CNN models at testing stage

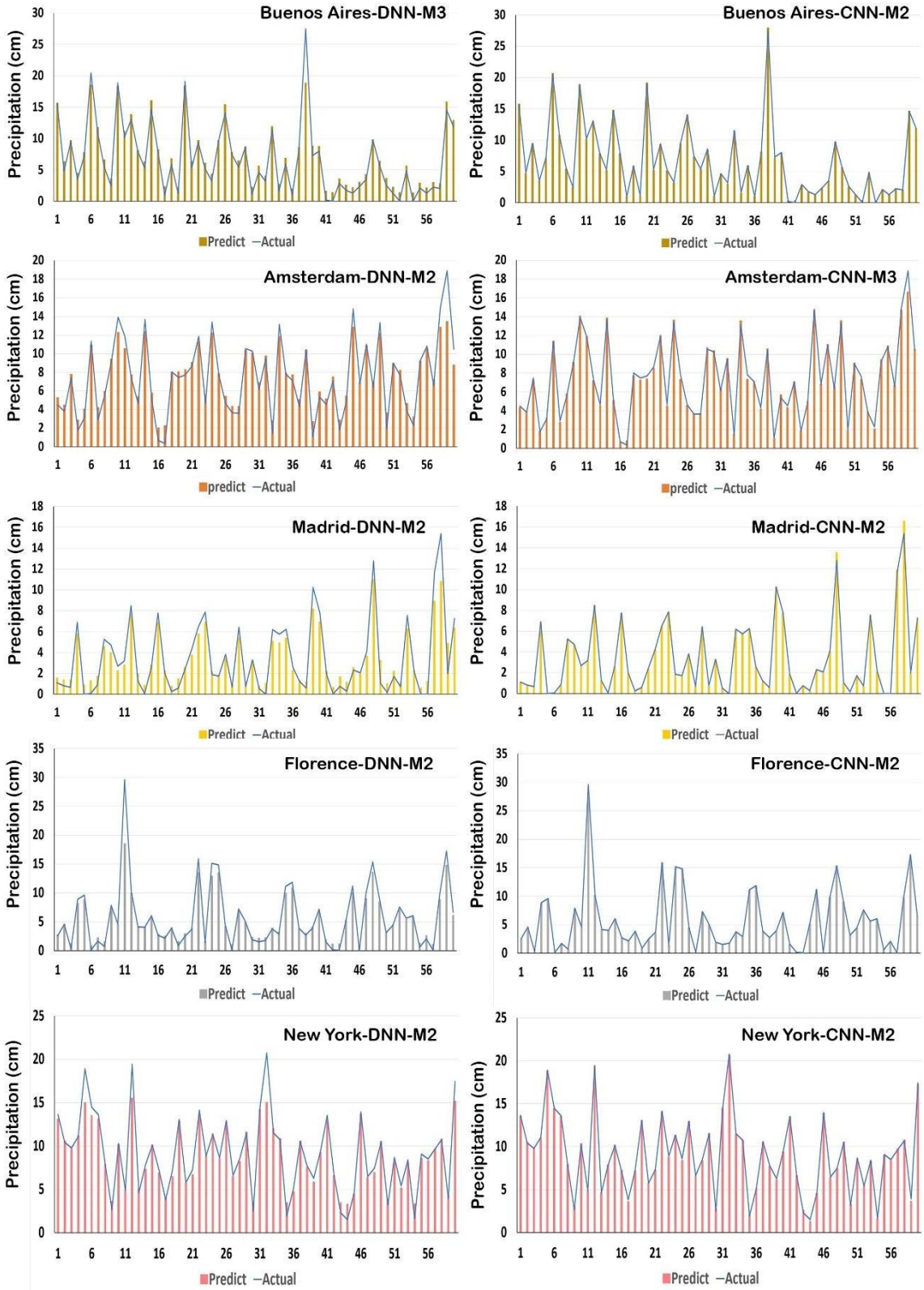


**Fig. 7** Time series for Buenos Aires, Amsterdam, Madrid, Florence, and New York best DNN and CNN models at testing stage

Also in **Fig. 8** are show box plots for ten cities. According to the box diagrams and the maximum, median, and minimum values for each city, it is possible to understand the high performance of the CNN model compared to DNN in predicting the precipitation parameter. Taking into account the confidence bands in **Fig. 9 and 10**, it can be observed that the CNN model demonstrates the highest level of precision ($R^2$ between 0.992, 0.999), whereas the DNN model displays a broader distribution of the measured and predicted MWSs ($R^2$ between 0.917, 0.978). CNN and DNN for each city show that the values predicted by the DNN model in some cities are within the confidence band and have good accuracy. Still, in general, the values predicted by the CNN model are within the band in all predictions and have a higher accuracy than the accuracy of the DNN model.

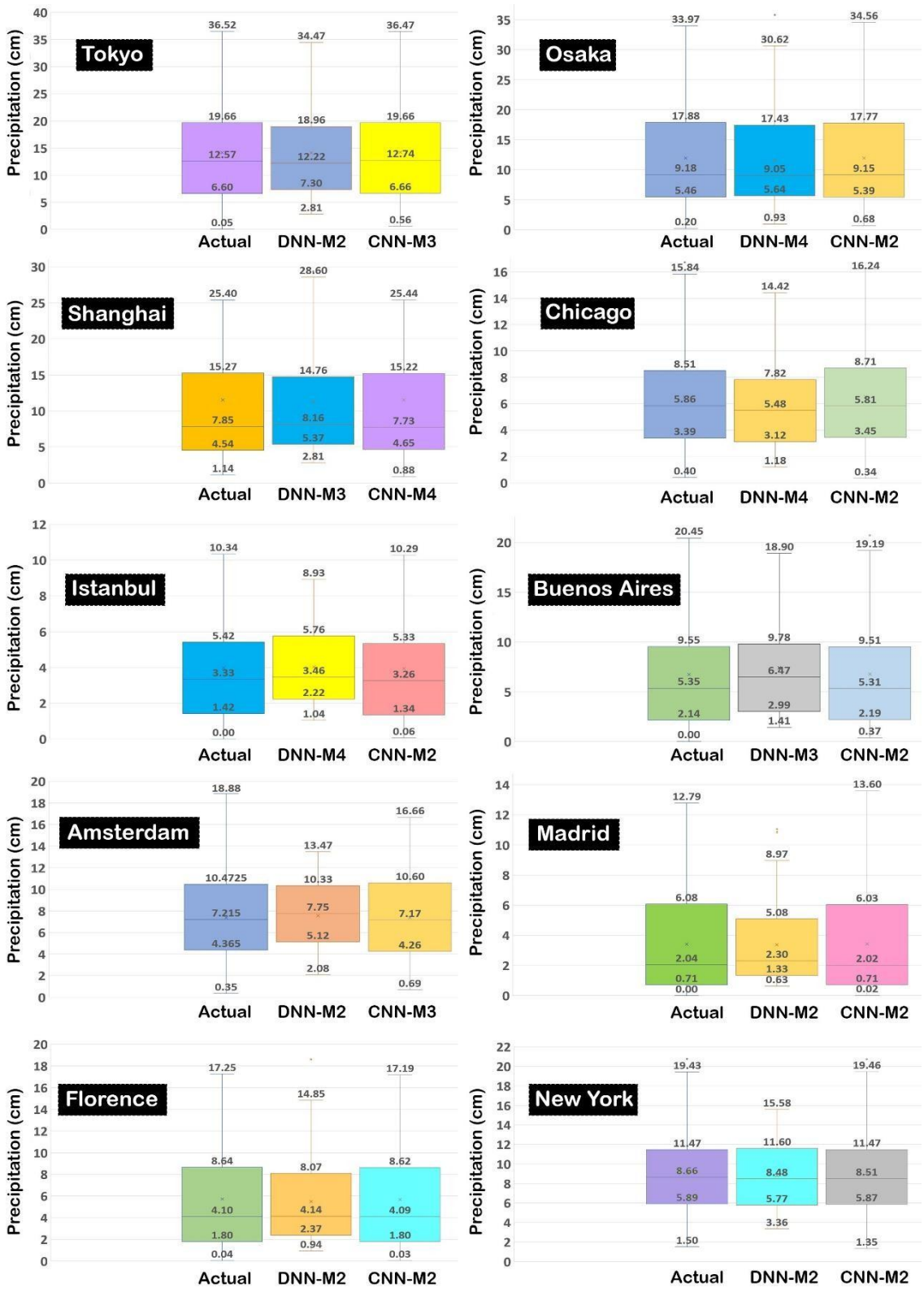


**Fig. 8** Box plot for ten important cities of the observed and predicted MP(t) for the best DNN and CNN models at testing stage

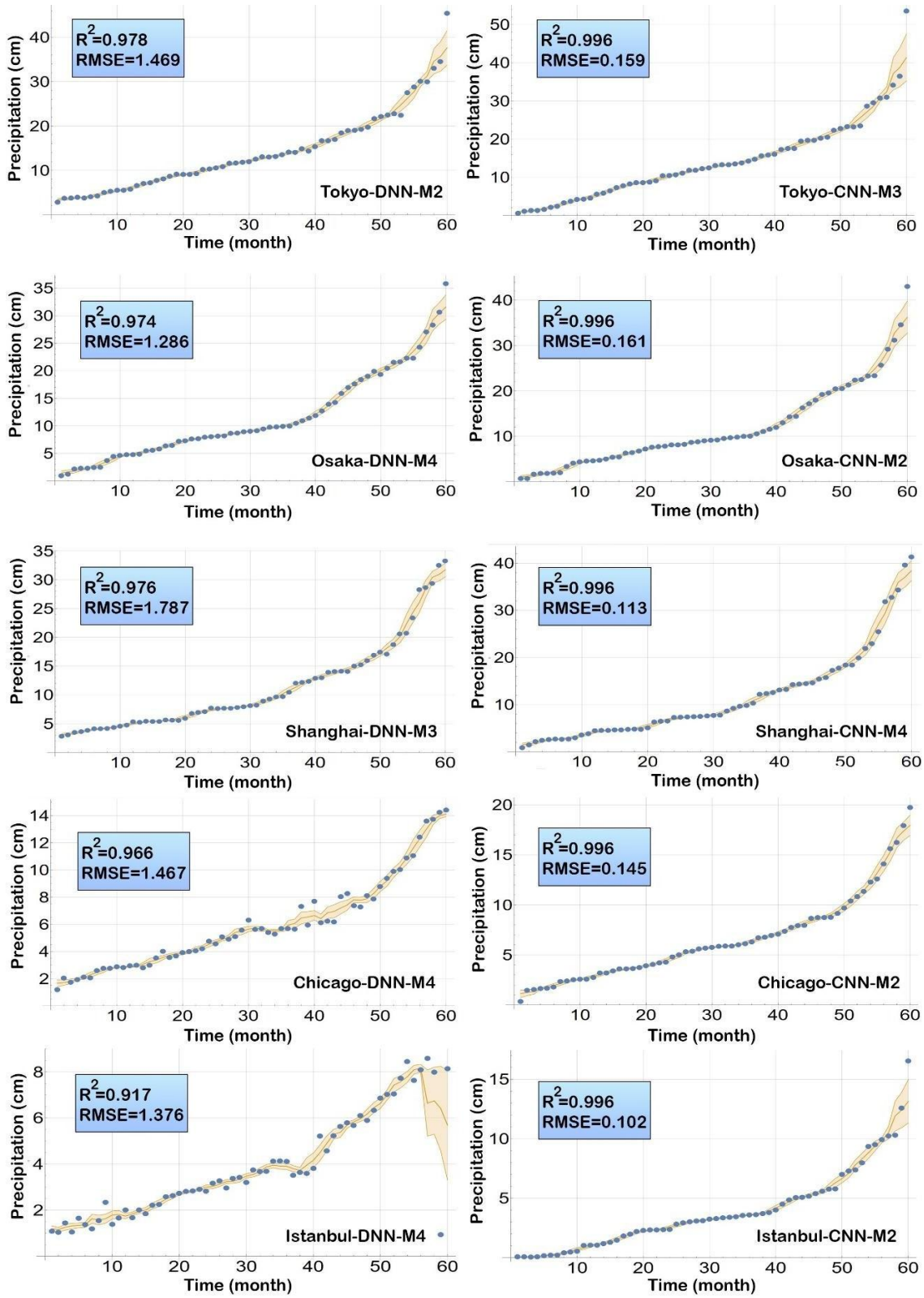


**Fig. 9** Confidence bands for Tokyo, Osaka, Shanghai, Chicago, and Istanbul best DNN and CNN models at testing stage

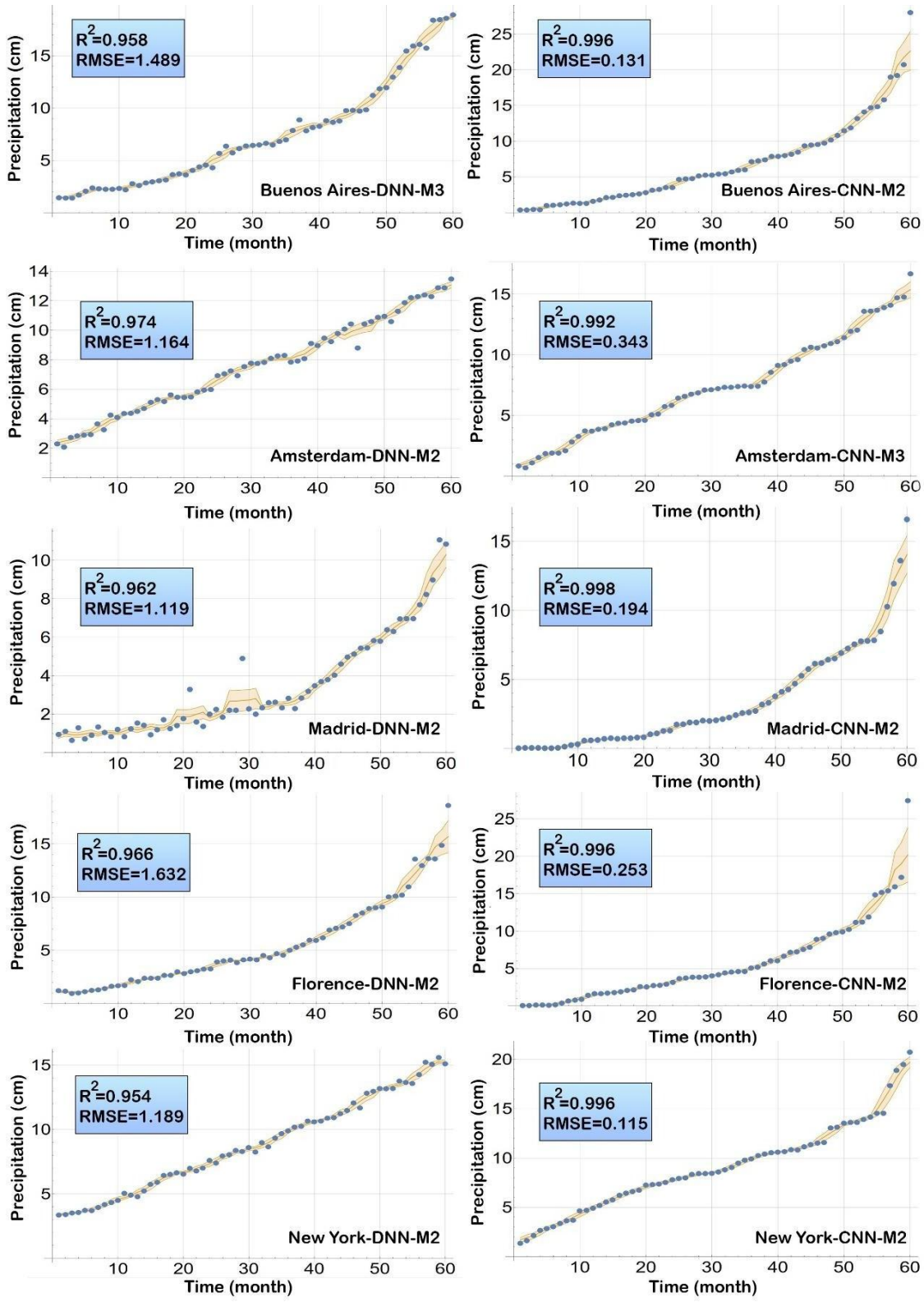


**Fig. 10** Confidence bands for Buenos Aires, Amsterdam, Madrid, Florence, and New York best DNN and CNN models at testing stage

### 3.2. Discussion

For the generation of precise Mean Precipitation forecasts, especially for the most extreme maximum and minimum values, the CNN model proved to be effective. Observing the statistical indicators and diverse graphical representations, it was noticed that when comparing the CNN model to the DNN model, the CNN model displayed superior performance in forecasting monthly mean precipitation in Tokyo, Osaka, Shanghai, Chicago, Istanbul, Buenos Aires, Amsterdam,

Madrid, Florance, and New York which are ten important cities in the world. CNNs use the same

set of weights for different parts of the input, which helps reduce the total number of parameters and prevents overfitting. The accuracy of this study is consistent with previous research where the implementation of a CNN model resulted in a significant increase in accuracy and a reduction in error (Sun et al. 2023; Kareem et al. 2021; Pan et al. 2019; Miao et al. 2019). It is important to note that limited research or analysis has been conducted on the implementation of the standalone CNN model to predict the MPs of ten particular cities.

Various studies utilized artificial neural networks (ANN) and soft computing methods to model and predict hydrologic processes, particularly precipitation dynamics (Lohani et al. 2006; Malik et al. 2021; Elbeltagi et al. 2022). Li et al (2022) Create a complex neural network incorporating both convolution and LSTM recurrent modules to predict precipitation using detailed atmospheric dynamic data. Sun (2023) A unique universe for CNN specifically for Performing several equations (MME) from CMIP6 monsoon rainfall over China in a local are Level. This framework is compared to 32 Global Climate Models (GCMs), along with Mainstream approaches such as quantitative mapping (QM) and rate set (ENS)Among other things, including linear regression after variables (MLR),, support vector machine (SVM), random forest (RF), and K-nearest neighbors (KNN), against in-situ measurements during 1970–

2014. Li et al (2020) For the purpose of obtaining the results of rainfall forecasts, Miley considered the following Improving the post-processing model based on convolutional neural networks (CNNs),Blending spatial information and atmospheric circulation variables as auxiliary predictions. The Post-processing model proposed to CNN demonstrates superior performance in induction Accuracy and reliability compared to classical methods, especially for strong rain. Based on The results of this study, it has been proven that ML mod

## 4. Conclusions

Accurate prediction of nonlinear processes, especially in the case of weather parameters like Precipitation that display intricate behavior influenced by factors including evapotranspiration and temperature, can be achieved through the utilization of ML techniques. Assessing the predictive potential of DNN and CNN models, this present investigation specifically targeted ten crucial cities for forecasting MP(t). Our preparation for the ML modeling process involved utilizing average mutual information (AMI), a nonlinear input variable selection method, to identify the dominant inputs among varied lag times of City MP up to a maximum lag period of 4 months. The performance of the two created models was assessed through an evaluation that considered statistical indicators like R and RMSE, as well as an analysis of statistical graphs. In regards to estimating mean precipitation, the CNN model proved its superiority over the DNN model by delivering superior outcomes for cities precipitation. In the pursuit of refining the structure of intelligent standalone models, upcoming research must give significant attention to employing CNN and corresponding hybrid methods for the prediction of various hydrological variables (e.g.temperature, wind speed, and evapotranspiration). Furthermore, performing comprehensive comparisons with algorithms is an improvement.

## References

Bauer, P., Thorpe, A., & Brunet, G. (2015). The quiet revolution of numerical weather prediction. *Nature*, *525*(7567), 47-55.

Chung, K. S., & Yao, I. A. (2020). Improving radar echo Lagrangian extrapolation nowcasting by blending numerical model wind information: Statistical performance of 16 typhoon cases. *Monthly Weather Review*, *148*(3), 1099-1120.

Chau, K. W., & Wu, C. L. (2010). A hybrid model coupled with singular spectrum analysis for daily rainfall prediction. *Journal of Hydroinformatics*, *12*(4), 458-473.

Dash, Y., Mishra, S. K., & Panigrahi, B. K. (2018). Rainfall prediction for the Kerala state of India using artificial intelligence approaches. *Computers & Electrical Engineering*, *70*, 66-73.

Dastorani, M., Mirzavand, M., Dastorani, M. T., & Sadatinejad, S. J. (2016). Comparative study among different time series models applied to monthly rainfall forecasting in semi-arid climate condition. *Natural Hazards*, *81*, 1811-1827.

Elbeltagi, A., Raza, A., Hu, Y., Al-Ansari, N., Kushwaha, N. L., Srivastava, A., ... & Zubair, M. (2022). Data intelligence and hybrid metaheuristic algorithms-based estimation of reference evapotranspiration. *Applied Water Science*, *12*(7), 152.

Foresti, L., Sideris, I. V., Nerini, D., Beusch, L., & Germann, U. (2019). Using a 10-year radar archive for nowcasting precipitation growth and decay: A probabilistic machine learning approach. *Weather and Forecasting*, *34*(5), 1547-1569.

Ghorbani M, Kahya E, Ruskeepää H, Roshni T, Kashani MH, Karimi V, Arikan BB (2022) Temporal connections in reconstructed monthly rainfall time series in different rainfall regimes of Turkey. Arab J Geosci 15: 1015

Kareem, S., Hamad, Z. J., & Askar, S. (2021). An evaluation of CNN and ANN in prediction weather forecasting: A review. *Sustainable Engineering and Innovation*, *3*(2), 148-159.

Kisi, O., & Cimen, M. (2012). Precipitation forecasting by using wavelet-support vector machine conjunction model. *Engineering Applications of Artificial Intelligence*, *25*(4), 783-792.

Krizhevsky, A., Sutskever, I., & Hinton, G. E. (2012). Imagenet classification with deep convolutional neural networks. *Advances in neural information processing systems*, *25*.

Li, P., Zhang, J., & Krebs, P. (2022). Prediction of flow based on a CNN-LSTM combined deep learning approach. *Water*, *14*(6), 993.

Li, W., Pan, B., Xia, J., & Duan, Q. (2022). Convolutional neural network-based statistical post-processing of ensemble precipitation forecasts. *Journal of hydrology*, *605*, 127301.

Li, G., Chang, W., & Yang, H. (2020). A novel combined prediction model for monthly mean precipitation with error correction strategy. *IEEE Access*, *8*, 141432-141445.

Liakos, K. G., Busato, P., Moshou, D., Pearson, S., & Bochtis, D. (2018). Machine learning in agriculture: A review. *Sensors*, *18*(8), 2674.

Lohani, A. K., Goel, N. K., & Bhatia, K. K. S. (2006). Takagi–Sugeno fuzzy inference system for modeling stage–discharge relationship. *Journal of Hydrology*, *331*(1-2), 146-160.

Malik, A., Tikhamarine, Y., Al-Ansari, N., Shahid, S., Sekhon, H. S., Pal, R. K., ... & Sammen, S.

S. (2021). Daily pan-evaporation estimation in different agro-climatic zones using novel hybrid support vector regression optimized by Salp swarm algorithm in conjunction with gamma test. *Engineering Applications of Computational Fluid Mechanics*, *15*(1), 1075-1094.

Miao, Q., Pan, B., Wang, H., Hsu, K., & Sorooshian, S. (2019). Improving monsoon precipitation prediction using combined convolutional and long short term memory neural network. *Water*, *11*(5), 977.

Milosevic, N., Corchero, M., Gad, A. F., & Michelucci, U. (2020). *Introduction to convolutional neural networks: with image classification using PyTorch*. Apress.

Maheswaran, R., & Khosa, R. (2014). A wavelet-based second order nonlinear model for forecasting monthly rainfall. *Water resources management*, *28*, 5411-5431.

Nerini, D., Foresti, L., Leuenberger, D., Robert, S., & Germann, U. (2019). A reduced-space ensemble Kalman filter approach for flow-dependent integration of radar extrapolation nowcasts and NWP precipitation ensembles. *Monthly Weather Review*, *147*(3), 987-1006.

Nourani, V., Alami, M. T., & Aminfar, M. H. (2009). A combined neural-wavelet model for prediction of Ligvanchai watershed precipitation. *Engineering Applications of Artificial Intelligence*, *22*(3), 466-472.

O'Shea, K., & Nash, R. (2015). An introduction to convolutional neural networks. *arXiv preprint arXiv:1511.08458*.

Pan, B., Hsu, K., AghaKouchak, A., & Sorooshian, S. (2019). Improving precipitation estimation using convolutional neural network. *Water Resources Research*, *55*(3), 2301-2321.

Papacharalampous, G., Tyralis, H., & Koutsoyiannis, D. (2019). Comparison of stochastic and machine learning methods for multi-step ahead forecasting of hydrological processes. *Stochastic environmental research and risk assessment*, *33*(2), 481-514.

Park, H. I., & Lee, S. R. (2011). Evaluation of the compression index of soils using an artificial neural network. *Computers and Geotechnics*, *38*(4), 472-481.

Pulkkinen, S., Nerini, D., Pérez Hortal, A. A., Velasco-Forero, C., Seed, A., Germann, U., & Foresti, L. (2019). Pysteps: An open-source Python library for probabilistic precipitation nowcasting (v1. 0). *Geoscientific Model Development*, *12*(10), 4185-4219.

Qiu, J., Shen, Z., Wei, G., Wang, G., Xie, H., & Lv, G. (2018). A systematic assessment of watershed-scale nonpoint source pollution during rainfall-runoff events in the Miyun Reservoir watershed. *Environmental Science and Pollution Research*, *25*, 6514-6531.

Ryu, S., Lyu, G., Do, Y., & Lee, G. (2020). Improved rainfall nowcasting using Burgers' equation. *Journal of Hydrology*, *581*, 124140.

Rezaie-Balf, M., Zahmatkesh, Z., & Kim, S. (2017). Soft computing techniques for rainfall-runoff simulation: local non–parametric paradigm vs. model classification methods. *Water Resources Management*, *31*, 3843-3865.

Ridwan, W. M., Sapitang, M., Aziz, A., Kushiar, K. F., Ahmed, A. N., & El-Shafie, A. (2021).

Rainfall forecasting model using machine learning methods: Case study Terengganu, Malaysia. *Ain Shams Engineering Journal*, *12*(2), 1651-1663.

Sammen, S. S., Ehteram, M., Abba, S. I., Abdulkadir, R. A., Ahmed, A. N., & El-Shafie, A. (2021). A new soft computing model for daily streamflow forecasting. *Stochastic Environmental Research and Risk Assessment*, *35*(12), 2479-2491.

Sønderby, C. K., Espeholt, L., Heek, J., Dehghani, M., Oliver, A., Salimans, T., ... & Kalchbrenner,

N. (2020). Metnet: A neural weather model for precipitation forecasting. *arXiv preprint arXiv:2003.12140*.

Sun, L., Lan, Y., & Jiang, R. (2023). Using CNN framework to improve multi-GCM ensemble predictions of monthly precipitation at local areas: An application over China and comparison with other methods. *Journal of Hydrology*, *623*, 129866.

Shi, X., Chen, Z., Wang, H., Yeung, D. Y., Wong, W. K., & Woo, W. C. (2015). Convolutional LSTM network: A machine learning approach for precipitation nowcasting. *Advances in neural information processing systems*, *28*. 802-810.

Ujong, J. A., Mbadike, E. M., & Alaneme, G. U. (2022). Prediction of cost and duration of building construction using artificial neural network. *Asian Journal of Civil Engineering*, *23*(7), 1117-1139.

Woo, W. C., & Wong, W. K. (2017). Operational application of optical flow techniques to radar-based rainfall nowcasting. *Atmosphere*, *8*(3), 48.

Wu, W., Guozhi, W., Yuanmin, Z., & Hongling, W. (2009, May). Genetic algorithm optimizing neural network for short-term load forecasting. In *2009 International Forum on Information Technology and Applications* (Vol. 1, pp. 583-585). IEEE.